Switching of a coupled spin pair in a single-molecule junction

Stefan Wagner[1], Ferdinand Kisslinger[1], Stefan Ballmann[1], Frank Schramm[2]*, Rajadurai Chandrasekar[2†], Tilmann Bodenstein[2], Olaf Fuhr[2], Daniel Secker[1], Karin Fink[2]*, Mario Ruben[2,3] and Heiko B. Weber[1]*

Single-molecule spintronics investigates electron transport through magnetic molecules that have an internal spin degree of freedom[1]. To understand and control these individual molecules it is important to read their spin state[2]. For unpaired spins, the Kondo effect has been observed[3-8] as a low-temperature anomaly at small voltages. Here, we show that a coupled spin pair in a single magnetic molecule can be detected[9,10] and that a bias voltage can be used to switch between two states of the molecule. In particular, we use the mechanically controlled break-junction technique[11] to measure electronic transport through a single-molecule junction containing two coupled spin centres that are confined on two Co^{2+} ions. Spin–orbit configuration interaction methods are used to calculate the combined spin system, where the ground state is found to be a pseudo-singlet and the first excitations behave as a pseudo-triplet. Experimentally, these states can be assigned to the absence and occurrence of a Kondo-like zero-bias anomaly in the low-temperature conductance data, respectively. By applying finite bias, we can repeatedly switch between the pseudo-singlet state and the pseudo-triplet state.

We have designed, synthesized and fully characterized a molecular complex **1** that has two coupled magnetic centres and was specifically intended for single-molecule experiments (Fig. 1a,b). We opted for a system in which the ion pair is not aligned in the current path, but the magnetic coupling path is orthogonally oriented to the conduction channel. The applied voltage will therefore affect the exchange coupling pathway and the local anisotropy, rather than the charge state of the magnetic ions. Structurally, this idea was implemented by tailoring a ligand molecule **L** (Fig. 1c), comprising a central coordination unit where two Co^{2+} ions are bonded side-on to the preferential axis of the co-planar bipyrimidine moiety, to form complex **1** (Fig. 1b; see Supplementary Section S1).

Such dicobalt systems are known for the delicate interplay of spin–orbit coupling, anisotropy and the bridging molecular structure[12]. In complex **1**, the Co^{2+} ions are found in a quasi-octahedral surrounding and a d^7 highspin configuration with $S = 3/2$. In this situation, different occupations of the d orbitals are energetically almost degenerate. The three-fold degeneracy of the $^4T_{1g}$ state, present in a perfect octahedron, is lifted by the ligand field and by spin–orbit coupling.

A reliable description of the electronic structure of complex **1** requires a multireference wavefunction-based method, where a linear combination of different occupations of the d orbitals is considered. We have performed complete active space self-consistent field calculations (CASSCF) and accounted for spin–orbit coupling by spin–orbit configuration interaction (SOCI) calculations on the lowest electronic states[13,14].

The results of our calculations are summarized in Fig. 1d. Because of the ligand field splitting, three $^4A_1$ states exist at each Co centre. The lowest $^4A_1$ shows a zero field splitting of 150 cm^{-1} into two Kramers doublets E_1 and E_2 due to spin–orbit coupling. Only the lowest Kramers doublet at each Co centre contributes to those electronic states of the binuclear complex that are accessible at low temperatures in a Boltzmann distribution. We therefore obtain four non-degenerate states including spin–orbit coupling, as shown in Fig. 1d (central column). Owing to the very weak spin coupling between the Co ions, the splitting is in the range of 2–3 cm^{-1} only.

In an external magnetic field the lowest state is not influenced. Depending on the field direction, two of the excited states show a typical Zeeman interaction while the third state remains constant. Although spin is not a good quantum number, the response to external magnetic fields (Fig. 3d) suggests an interpretation as a pseudo-singlet (no interaction with the magnetic field) and a pseudo-triplet state with additional zero field splitting. The ordering of the four states is typical for a very weak antiferromagnetic coupling mode, in agreement with the bulk magnetic data.

In directions perpendicular to the backbone, which are relevant for the experiment where only the orientation of the backbone is well controlled, g-values between 2 and 4 were calculated (Supplementary Section S6). Hence, at low measurement temperatures we expect the molecule to be in the pseudo-singlet state. With subtle parameter variations, a shift of the ground state to the pseudo-triplet state (Fig. 1d) is conceivable. Such a transition has been proposed as a consequence of an electric field[9], but could also be achieved by application of a magnetic field or subtle changes to the local environment.

In the present work, single-molecule contacts are indicated by nonlinear current–voltage ($I–V$) characteristics in ∼30% of the devices. For reference, we investigated the backbone of complex **1**, ligand **L** (Fig. 1c). Its $I–V$ characteristics did show a very similar behaviour (Supplementary Section S4), but no zero-bias anomaly (ZBA) and no dependence on the magnetic field.

We investigated the $I–V$ characteristics of molecule **1** at low temperatures. From measurements of many samples (we measured ten bridges, from which more than 30 atomically different junctions were established by opening and closing the electrode pair), we repeatedly found two qualitatively different phenomenologies, which we term type I and II data. We will first discuss the type I data, which show a specific feature that we never observe for measurements on non-magnetic molecules such as ligand **L**: a

[1]Lehrstuhl für Angewandte Physik, Friedrich-Alexander-Universität Erlangen-Nürnberg, Staudtstrasse 7, D-91058 Erlangen, Germany, [2]Institut für Nanotechnologie, Karlsruher Institut für Technologie (KIT), PF 3640, D-76021 Karlsruhe, Germany, [3]IPCMS, CNRS-Université de Strasbourg, 34 rue de Loess, F-67034 Strasbourg, France; [†]Present address: School of Chemistry, University of Hyderabad, Hyderabad-500 046, India.
*e-mail: frank.schramm@kit.edu; karin.fink@kit.edu; heiko.weber@physik.uni-erlangen.de
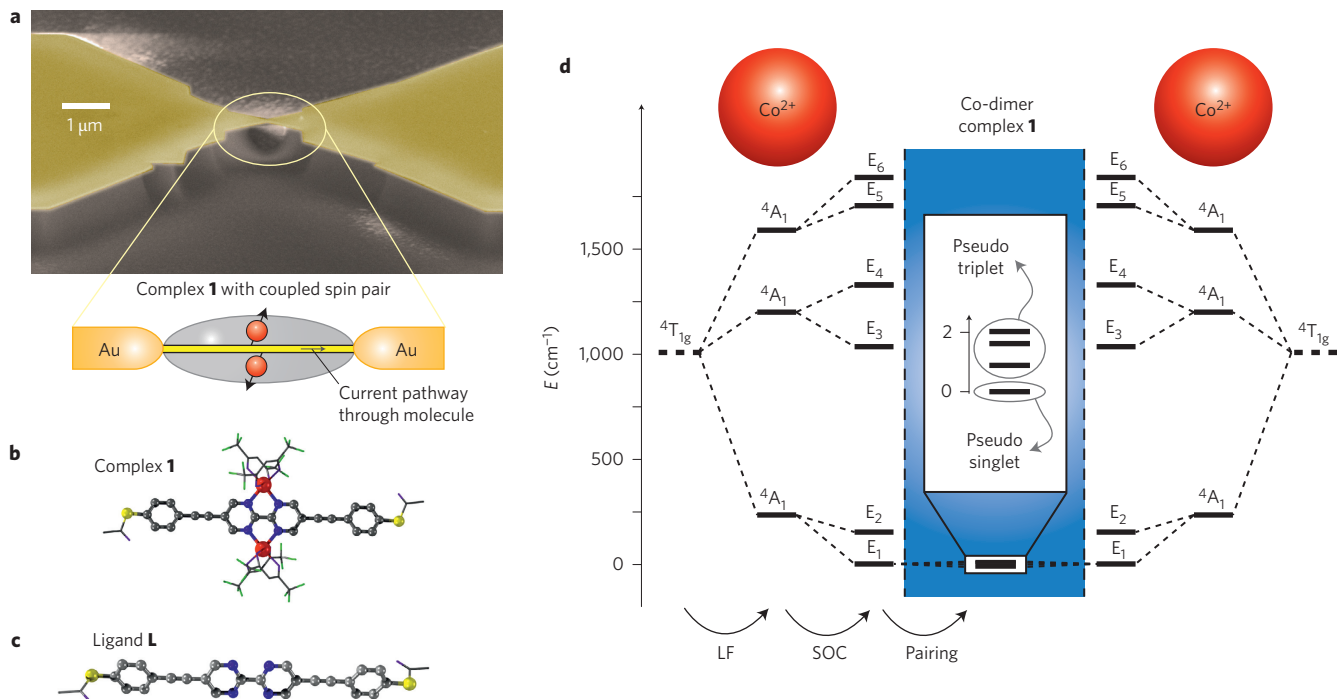
Figure 1 | Coupled spin pair in a break junction. a, Scheme of the experiment. A molecule with a pair of spin centres is contacted in a single-molecule junction (SEM micrograph of a break junction set-up). The magnetic ion pair is attached orthogonally to the current pathway. **b**, Molecular structure of complex **1** from single-crystal X-ray diffraction. The Co^{2+} ions are marked in red, carbon in grey, nitrogen in blue, oxygen in violet and sulphur in yellow; hydrogen atoms are omitted for clarity. **c**, Molecular structure of bare bipyrimidine-wire **L** (for control experiments) from single-crystal X-ray diffraction. **d**, Electronic states of the coupled spin system, as obtained from quantum chemical calculations. First column: Co^{2+} in octahedral surrounding ($^4T_{1g}$). Second column: splitting as a consequence of the ligand field in complex **1**. Third column: influence of spin–orbit coupling. The central column indicates the consequence of pairing the Co centres: a pseudo-singlet and a pseudo-triplet state, which is further split by zero-field splitting.

finite slope at zero bias, which appears as a peak in dI/dV (Fig. 2a). This ZBA, roughly Lorentzian in shape, becomes narrower and higher at lower temperatures. We will assign this ZBA to the Kondo effect, which relates to the many-body interaction of conduction electrons with a magnetic degree of freedom. The Kondo effect is associated with a logarithmic increase in conductance G_{max} towards lower temperatures and a peak splitting in magnetic fields. Accordingly, we analysed the temperature dependence.

For a closer characterization, we adapted Lorentzians to the ZBA, and plotted the resulting values for peak height G_{max} and peak width as a function of temperature (Fig. 2b,c). It turns out that $dI/dV(T,V)$ follows the well-known Kondo behaviour, where the conductance maximum increases logarithmically towards low temperatures up to a saturation value, as can be seen in Fig. 2b. The data fit well to the models

$$G_{max}(T) = G_C + G_0(1 + (2^{1/s} - 1)(T/T_K)^2)^{-s}$$

and

$$\Lambda_{FWHM} = g_0 \cdot \sqrt{(\pi k_B T)^2 + 2(k_B T_K)^2}$$

for the temperature dependence of the conductance maximum $G_{max}(T)$ (ref. 15) and the full-width at half-maximum $\Lambda_{FWHM}(T)$ (Fig. 2b,c)[16], where G_C is an offset value, G_0 is the conductance range, g_0 is a dimensionless parameter, T_K is the characteristic Kondo temperature, and s is the spin parameter (0.22 for spin 1/2, the simplest case). The fit yields $T_K = 5.0$ K using the G_{max} equation and $s = 0.20$ and $T_K = 1.4$ K using the Λ_{FWHM} model. Note that the most fundamental model of spin 1/2 is
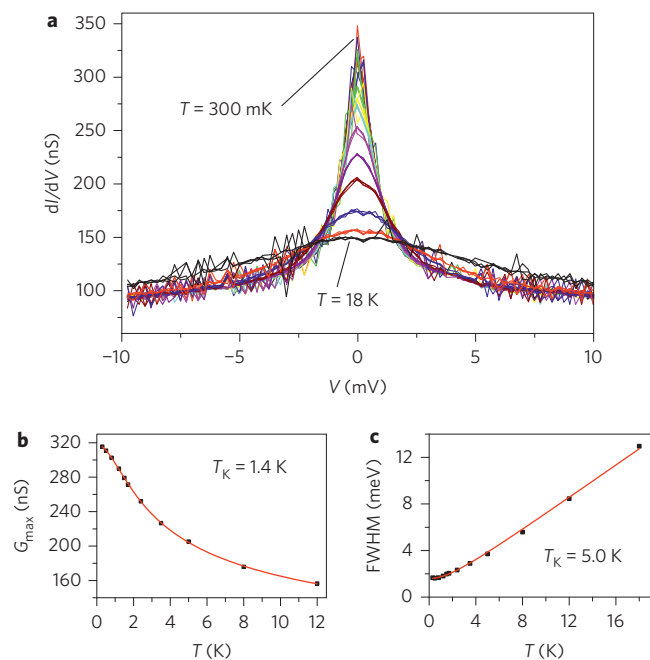

Figure 2 | Molecular junctions of type I, with Kondo-like behaviour. a, Temperature dependence of the Kondo-like feature (similar to Fig. 4a). **b**, $T_K = 1.4$ K, from a fit of the Kondo model (continuous line) to the data (black points) of the conductance maximum at zero bias. **c**, FWHM measured versus temperature (black data points), fit by a Kondo model (continuous line), giving $T_K = 5.0$ K.
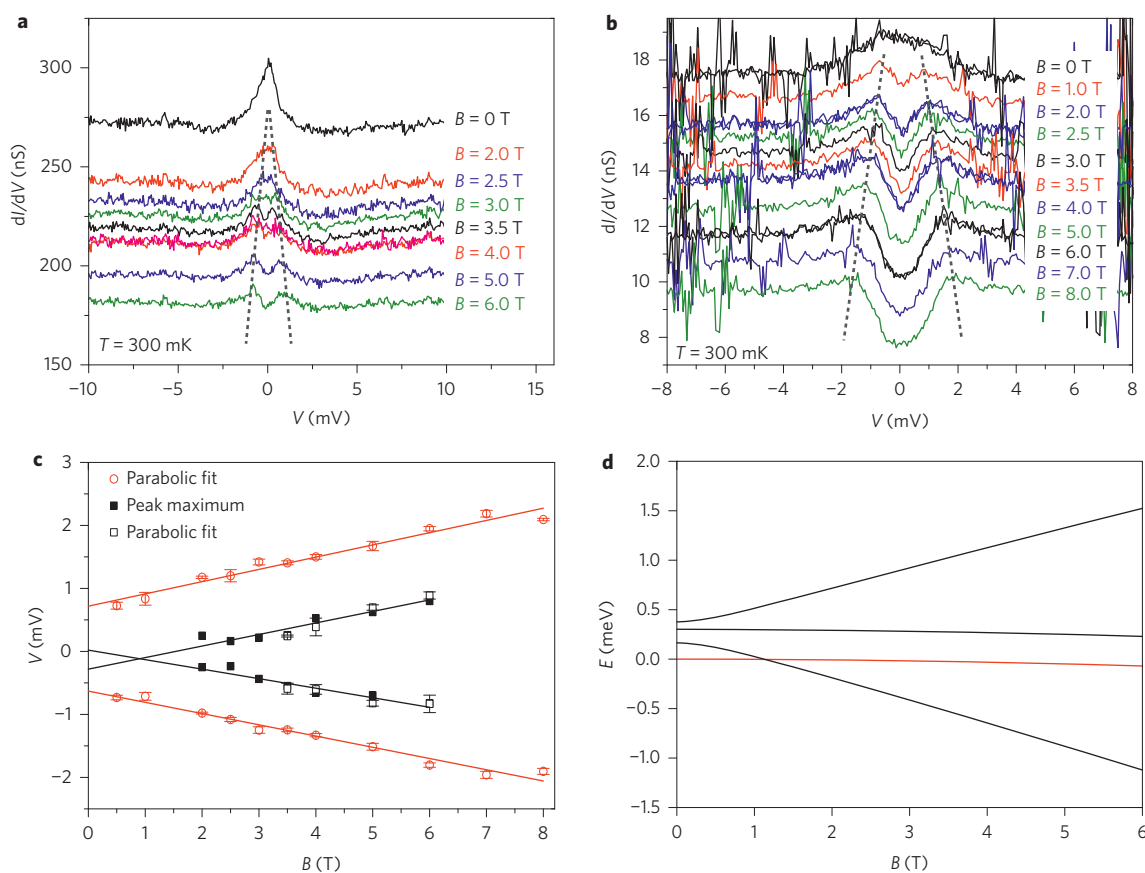
Figure 3 | Magnetic-field dependence of the ZBA for two different samples. a,b, The zero-bias peak (assigned to a pseudo-triplet state) splits linearly with magnetic fields B and forms a symmetric double peak structure, as expected for a Kondo feature. This confirms the assignment to a magnetic degree of freedom. **c**, Peak positions plotted versus magnetic field. Error bars indicate the statistical error when locally adapting parabola to the peaks. The slope of the curves allows the g-factors to be determined ($g = 2.6$–3.3). **d**, Calculated response of the pseudo-singlet (red) and the pseudo-triplet (black) states to a magnetic field applied along the direction of the two Co ions yield a g-factor of 3.3. This agrees reasonably well with the values obtained in **c**.

considered here. It is known, however, that higher spin values often yield similar phenomena, in particular in the presence of magnetic anisotropy[17–21].

However, it remains unresolved why the saturation value of the conductance is far below the expected conductance quantum $G_0 \approx 77.5\ \mu S$, which is a consequence of perfect transmission in the unitary limit. It is at least conceivable that the saturation at the lowest temperatures may be caused by insufficient local thermalization or insufficient Kondo screening. In this case, the determined Kondo temperatures would be overestimated.

At this point, we refer to the electronic structure calculations. Given the even number of electrons and the two nearly degenerate magnetic states, this Kondo-like peak is an indicator of the described pseudo-triplet state. An important check is whether the Kondo-like anomaly indeed has a magnetic origin. We therefore exposed the sample to magnetic fields orientated perpendicular to the junction axis. The mechanically controlled break junction technique (MCBJ) has an advantage over other methods of nanojunction fabrication in that the molecule's axis can be well controlled by stretching the junction.

For some samples displaying a Kondo-like ZBA (type I) we could find a field splitting, as predicted for Kondo anomalies[8,17]. Other junctions became unstable when magnetic fields were applied. Figure 3a,b presents the ZBA at the lowest temperature ($T = 300$ mK) for two different junctions. The ZBA splits and moves outwards with increasing fields. An analysis of the peak positions as a function of magnetic field B is displayed in Fig. 3c,d. Despite the experimental uncertainties in the peak positions, the

data fit reasonably well to a straight line, with a slope given by the Zeeman splitting of the pseudo-triplet states ($S = 1$). The analysis also gives a g-factor of ~2.6–3.3, which agrees well with the theoretical values perpendicular to the backbone. For ligand **L**, no response to the magnetic field was observed.

Another typical type I I–V characteristic with a Kondo-like anomaly similar to that in Fig. 2 is shown in Fig. 4a. Apart from the ZBA, it exhibits no special features up to ± 1 V. Note that the amplitude of this Kondo-like anomaly varies significantly from sample to sample.

We now focus on the second set of typical I–V characteristics observed (type II). One example is presented in Fig. 4b. Remarkably, there is no Kondo-like anomaly. At first sight this curve looks similar to the data observed with other molecules, with an onset of current well beyond 0.5 V. However, a striking feature occurs in the low-bias regime: at $V_{th} \approx \pm 0.2$ V, a symmetric current step indicates a transition that is different from resonant tunnelling. A closer look at the dI/dV curve (Fig. 4b, lower panel) reveals strong fluctuations, rather untypical for an electronic resonance, which would generate a smooth, broad peak at bias voltages of a few hundred millivolts[22]. For that reason we ascribe the transition at $|V_{th}|$ to a sudden but subtle switch of the system. This behaviour is found in many junctions. As we can see no Kondo-like anomaly and no response to the magnetic field in these curves, we assign the type II behaviour to the non-magnetic pseudo-singlet state of the molecule.

We have learned in the past that pulling and pushing the electrodes often results in changes to the I–V characteristics[11,23]. We
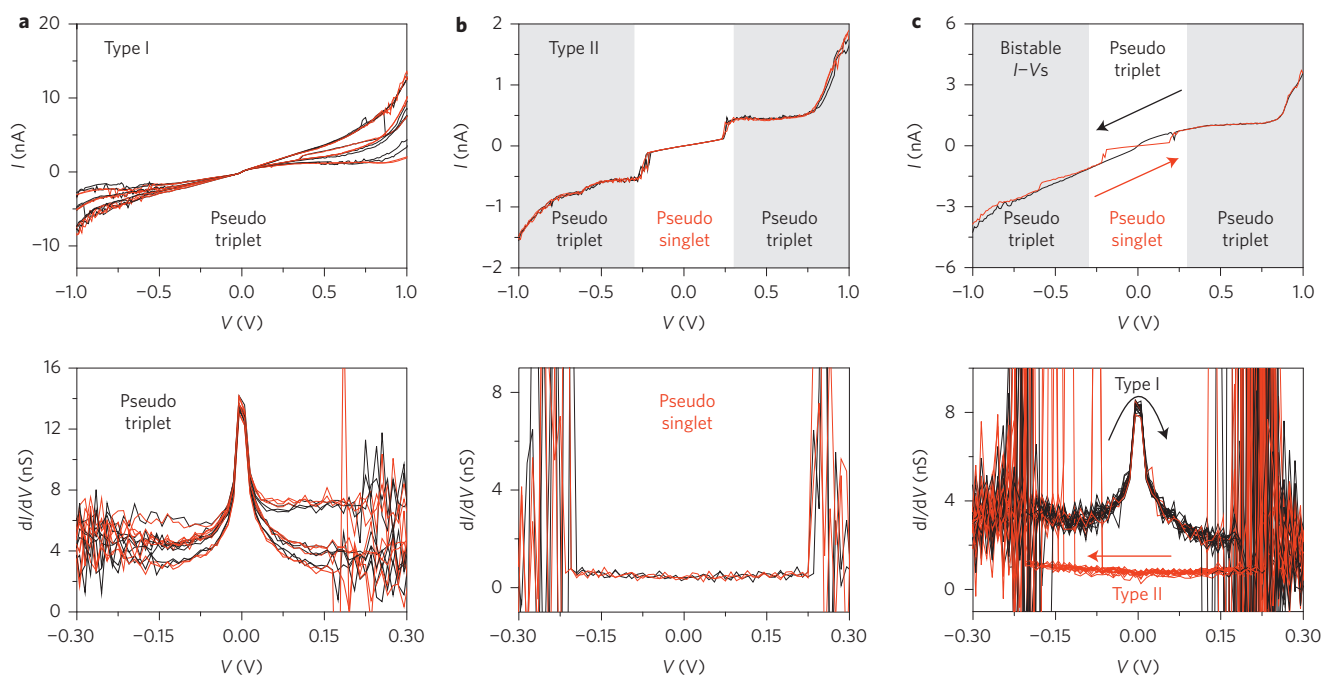
Figure 4 | I–V characteristics recorded at low temperatures and the corresponding differential conductance obtained by numerical differentiation. Up-sweeps are marked in black and down-sweeps in red. **a**, Many curves display a Kondo-like zero bias anomaly, but no discontinuity. We classify this I–V behaviour as type I. This is identified as the electrical fingerprint of the pseudo-triplet state. **b**, Another frequently occurring set of data displays no Kondo-like anomaly, but a discontinuity at ∼0.2 V. These I–V characteristics are termed type II. We assign the inner part to the pseudo singlet. Assignment of the outer part to the pseudo triplet state becomes clear in **c**. **c**, Bistable I–V characteristics due to hysteresis of the coupled spin pair. Down-sweeps are similar to **b** and up-sweeps to **a**. The data in **c** were recorded immediately after **b**. This behaviour was reproduced over 24 sweeps and occurred in three samples.

therefore varied the electrode spacing for the particular junction described in Fig. 4b. The subsequent measurement with approached contacts is particularly well suited to clarifying the correspondence between the two sets of I–V characteristics reported so far. Remarkably, an additional feature occurs, which affects only the small bias region: a bistable regime in the range $|V| \lesssim 0.2$ V (Fig. 4c).

When the voltage is lower than −0.2 V the system switches to the triplet state. During the up-sweeps (towards positive voltages, black line), the discontinuity is suppressed and a ZBA (as in type I data) appears. When sweeping down (red line), the aforementioned line shape with the discrete transition is recovered (type II). In particular, no ZBA occurs in this case. This behaviour was subsequently reproduced (only three exceptions in 24 sweeps, and the switching is always correlated with the absence of a ZBA). In all single-molecule junctions we observe either type I or type II lineshapes (Fig. 4a,b, respectively), except for an occasional bistable state. This latter state was observed in four independent samples.

The bistable case includes type I and type II data in a single curve and thus gives access to how the two line shapes are related to one another. The type I data, which we can assign to the triplet state due to the Kondo-like ZBA, is continuous in the given bias range. The type II curve, which has no ZBA and is assigned to the singlet state, is discontinuous at V_{th}, and it switches to a curve that is identical to the type I curve. Accordingly, the bistable curve links the two regimes, and the switching in Fig. 4b can be interpreted as a transition from the non-magnetic pseudo singlet at low bias to the pseudo triplet at high bias, as indicated by the shaded areas in Fig. 4b,c. Note that Fig. 4c was recorded immediately after Fig. 4b at the same junction, which underwent only a minute change.

The microscopic origin of the bias-induced switching is not easy to pinpoint. An electric field-induced asymmetry has been proposed as a driving force for singlet–multiplet transitions in a dicobalt system[9]. In our case, the two magnetic sites are approximately on the same equipotential line, when assuming symmetric electrodes.

Nevertheless, due to the irregular shape of the junction on the atomic scale there are many potential causes of asymmetries, which may act on bonding angles, the charge distribution on the molecule, and so on. In particular, the applied bias redistributes the charge on the conjugated wire, which affects the magnetic exchange pathway between the Co sites[24].

Although the assignment of the Kondo anomaly to the triplet state is convincing, an unambiguous assignment of the absence of a Kondo anomaly to the singlet state is difficult. For example, the transition could also be assigned to a sudden drop in the Kondo temperature, such that an eventual magnetic degree of freedom is undetectable.

In conclusion, we have found a bias-driven switching that we have assigned to the transition from the pseudo-singlet ground state of a coupled spin system to a pseudo-triplet state at higher bias voltage. This is identified by a bistability that occurred in four samples.

By decreasing the bias from above $V \approx 0.2$ V, the reverse transition from pseudo-triplet to pseudo-singlet state did not occur for one of the orientations of the bias voltage. Instead a Kondo anomaly at zero bias indicated a non-vanishing magnetic moment at even electron numbers. Thus, the experiment indicates a singlet–multiplet transition of a magnetic molecule in a single-molecule conductance experiment.

Methods

All reagents and solvents used in this study are commercially available and were used without further purification. NMR spectroscopic data were recorded with a Bruker DPX 300 or on a Bruker AC 500 spectrometer. Infrared spectra were recorded using KBr-pressed pellets with a Perkin-Elmer Spectrum GX Fourier-transform infrared spectrometer. Matrix-assisted laser desorption/ionization time of flight mass spectrometry data were acquired with a Voyager-DE PRO Bio spectrometry workstation. Elemental analyses were carried out with a Vario Micro cube.

X-ray crystallographic studies for ligand **L** were carried out at beamline ID11 at the European Synchrotron Radiation Facility (ESRF). X-ray crystallographic data

collection for complex **1** was performed with a STOE IPDS II diffractometer. The temperature-dependent static susceptibilies of **1** were recorded with an MPMS-5S (Quantum Design) SQUID magnetometer.

We used a mechanically controlled break junction set-up (Fig. 1a) in a ^{3}He refrigerator (sample in vacuum, 0.3–20 K). A magnetic field up to ± 8 T was available. The single-molecule contacts were stable for days if the bias voltage was limited to $\sim$200 mV, and stable for minutes and up to hours beyond this threshold. The application of molecules and the formation of single-molecule contacts is described in refs 11 and 25. None of the control experiments with bare gold junctions or only solvent demonstrated molecular $I-V$ characteristics.

For the quantum-chemical calculations, the CASSCF and SOCI program of the Bochum set of *ab initio* programs was used[13,26]. All atoms were equipped with a def2-SV basis set[27]. The Co basis set was modified slightly (the contraction scheme of the d-function was changed from [4,1] to [3,1,1], a semidiffuse p-function was added, and the most diffuse s-function removed). At the N and O ligand atoms the basis set was extended to def2-SVP. In the CASSCF calculations for the binuclear complex the 3*d* orbitals of the Co ions occupied with 14 electrons were chosen as the active space. In the SOCI calculations the spin–orbit interaction of the first 36 states (nine singlets, triplets, quintets and septets, respectively) was included. According to this, five 3*d* orbitals with seven electrons were considered in the model complex with one Co ion, and the SOCI calculation was based on the three lowest quartet states.

References

1. Sanvito, S. Molecular spintronics. *Chem. Soc. Rev.* **40,** 3336–3355 (2011).
2. Schmaus, S. *et al.* Giant magnetoresistance through a single molecule. *Nature Nanotech.* **6,** 185–189 (2011).
3. Iancu, V., Deshpande, A. & Hla, S-W. Manipulation of the Kondo effect via two-dimensional molecular assembly. *Phys. Rev. Lett.* **97,** 266603 (2006).
4. Parks, J. J. *et al.* Tuning the Kondo effect with a mechanically controllable break junction. *Phys. Rev. Lett.* **99,** 026601 (2007).
5. Osorio, E. A. *et al.* Electrical manipulation of spin states in a single electrostatically gated transition-metal complex. *Nano Lett.* **10,** 105–110 (2010).
6. Park, J. *et al.* Coulomb blockade and the Kondo effect in single-atom transistors. *Nature* **417,** 722–725 (2002).
7. Liang, W., Shores, M. P., Bockrath, M., Long, J. R. & Park, H. Kondo resonance in a single-molecule transistor. *Nature* **417,** 725–729 (2002).
8. Meir, Y., Wingreen, N. S. & Lee, P. A. Low-temperature transport through a quantum dot: the Anderson model out of equilibrium. *Phys. Rev. Lett.* **70,** 2601–2604 (1993).
9. Baadji, N. *et al.* Electrostatic spin crossover effect in polar magnetic molecules. *Nature Mater.* **8,** 813–817 (2009).
10. Lehmann, J., Gaita-Arino, A., Coronado, E. & Loss, D. Spin qubits with electrically gated polyoxometalate molecules. *Nature Nanotech.* **2,** 312–315 (2007).
11. Reichert, J. *et al.* Driving current through single organic molecules. *Phys. Rev. Lett.* **88,** 176804 (2002).
12. Palii, A., Tsukerblat, B., Clemente-Juan, J. M. & Coronado, E. Magnetic exchange between metal ions with unquenched orbital angular momenta: basic concepts and relevance to molecular magnetism. *Int. Rev. Phys. Chem.* **29,** 135–230 (2010).
13. Fink, K., Wang, C. & Staemmler, V. Superexchange and spin–orbit coupling in chlorine-bridged binuclear cobalt(II) complexes. *Inorg. Chem.* **38,** 3847–3856 (1999).
14. Staemmler, V. & Fink, K. An *ab initio* cluster study of the magnetic properties of the CoO(0 0 1) surface. *Chem. Phys.* **278,** 79–87 (2002).
15. Costi, T. A., Hewson, A. C. & Zlatić, V. Transport coefficients of the Anderson model via the numerical renormalization group. *J. Phys. Condens. Matter* **6,** 2519–2558 (1994).
16. Nagaoka, K., Jamneala, T., Grobis, M. & Crommie, M. F. Temperature dependence of a single Kondo impurity. *Phys. Rev. Lett.* **88,** 077205 (2002).
17. Parks, J. J. *et al.* Mechanical control of spin states in spin-1 molecules and the underscreened Kondo effect. *Science* **328,** 1370–1373 (2010).
18. Hirjibehedin, C. F. *et al.* Large magnetic anisotropy of a single atomic spin embedded in a surface molecular network. *Science* **317,** 1199–1203 (2007).
19. Costi, T. A. *et al.* Kondo decoherence: finding the right spin model for iron impurities in gold and silver. *Phys. Rev. Lett.* **102,** 056802 (2009).
20. Romeike, C., Wegewijs, M. R., Hofstetter, W. & Schoeller, H. Quantum-tunneling-induced Kondo effect in single molecular magnets. *Phys. Rev. Lett.* **96,** 196601 (2006).
21. Romeike, C., Wegewijs, M. R., Ruben, M., Wenzel, W. & Schöller, M. Charge switchable molecular magnet and spin blockade of tunneling. *Phys. Rev. B* **77,** 064404 (2007).
22. Secker, D. *et al.* Resonant vibrations, peak broadening, and noise in single-molecule contacts: the nature of the first conductance peak. *Phys. Rev. Lett.* **106,** 136807 (2011).
23. Ruben, M. *et al.* Charge transport through a Cardan-joint molecule. *Small* **4,** 2229–2234 (2008).
24. Elbing, M. *et al.* A single-molecule diode. *Proc. Natl Acad. Sci. USA* **102,** 8815–8820 (2005).
25. Reed, M. A., Zhou, C., Muller, C. J., Burgin, T. P. & Tour, J. M. Conductance of a molecular junction. *Science* **278,** 252–254 (1997).
26. Meier, U. & Staemmler, V. An efficient first-order CASSCF method based on the renormalized Fock-operator technique. *Theor. Chim. Acta.* **76,** 95–111 (1989).
27. Weigend, F. & Ahlrichs, R. Balanced basis sets of split valence, triple zeta valence and quadruple zeta valence quality for H to Rn: design and assessment of accuracy. *Phys. Chem. Chem. Phys.* **7,** 3297–3305 (2005).

Acknowledgements

Author contributions

M.R. and H.B.W. conceived and designed the experiments. S.W., F.K. and S.B. performed the MCBJ experiments. Synthesis and full characterization of the chemicals were performed by R.C. (ligand **L**) and F.S. (complex **1**). Quantum-chemical calculations were performed and analysed by T.B. and K.F. O.F. determined the single-crystal X-ray data of complex **1**. S.W., F.K., S.B., F.S., T.B., K.F., M.R. and H.B.W. co-wrote the paper. All authors discussed and commented on the manuscript.

Additional information

Supplementary information is available in the online version of the paper. Reprints and permissions information is available online at www.nature.com/reprints. Correspondence and requests for materials should be addressed to F.S. (synthesis), K.F. (theory) and H.B.W. (experiment).

Competing financial interests

The authors declare no competing financial interests.